THE LINE PROFILE OF H LYMAN-a FROM DISSOCIATIVE EXCITATION OF H_2

JOSEPH M. AJELLO
ISIK KANIK
SYED M. AHMED

JET PROPULSION LABORATORY
CALIFORNIA INSTITUTE OF TECHNOLOGY
PASADENA, CALIFORNIA 91109

JOHN T. CLARKE
DEPARTMENT OF ATMOSPHERIC, OCEANIC AND SPACE SCIENCES
UNIVERSITY OF MICHIGAN
ANN ARBOR, MICHIGAN 48109

SUBMITTED TO :
JOURNAL OF GEOPHYSICAL RESEARCH

APRIL 1, 1995

ABSTRACT

A high-resolution ultraviolet (UV) spectrometer was employed for the first measurement of the H Lyman-a (H Lα) emission Doppler profile from dissociative excitation of H_2 by electron impact. Analysis of the deconvolved line profile reveals the existence of a narrow central peak of 40 ± 4 mÅ FWHM and a broad pedestal base about 240 mÅ wide. Three distinct dissociation mechanisms account for this Doppler structure. Slow H(2p) atoms characterized by a distribution function with peak energy near 80 meV produce the peak profile, which is nearly independent of the electron impact energy. Slow H(2p) atoms arise from direct dissociation and predissociation of singly excited states which have a dissociation limit of 14.68 eV. The wings of H Lα arise from dissociative excitation of a series of doubly excited states which cross the Franck-Condon region between 23 and 40 eV. The profile of the wings is dependent on the electron impact energy, and the distribution function of fast H(2p) atoms is, therefore, dependent on the electron impact energy. The fast-atom kinetic energy distribution at 100 eV electron impact energy spans the energy range from 1-10 eV with a peak near 4 eV. For impact energies above 23 eV the fast atoms contribute to a slightly asymmetric structure of the line profile. A third type of dissociation process is found from the observation of a threshold for cascade from the Balmer-α line. The absolute cross sections of the H Lα line peak and wings were measured over the range from 0-200 eV. Analytic model coefficients are given for the measured cross sections which can be applied to planetary atmosphere auroral and dayglow calculations.

* meV means milli-electron volt. Should it be MeV?
(Omega)

INTRODUCTION

H Lα line emission through dissociative excitation of H_2 is an important process in the upper atmospheres of the outer planets. The most prominent emission line in the uv airglow and aurora of the four outer planets, whose atmospheres are dominated by hydrogen, is H Let (Broadfoot et al., 1979, 1986, 1989). Following the first u v spectra of Jupiter's aurora and airglow by the Voyager u v spectrometer (Broadfoot et al., 1979) and the International Ultraviolet Explorer(IUE) (Clarke et al., 1980), it became clear that energy outputs of 10^{13} - 1014 W&-were present in the form of electron excitation in Jupiter's aurora (several orders of magnitude greater than in the Earth's aurora). The excitation yielded H Lα emissions of the order of 100 kR brightness, and the anticipated yield of superthermal H atoms by dissociative excitation of H_2 could then contribute to the dynamics of Jupiter's upper atmosphere. The first measurement of Jupiter's aurora] H Lα line profile was performed with the IUE at 0.14 -Å resolution in an attempt to detect the Doppler signature of precipitating fast protons, which would produce a pronounced red-shifted emission component from fast proton charge exchange into an excited state and subsequent radiation. The IUE auroral spectra showed no indication of such proton auroral emissions at redshifts of 1-2 Å. However, they did reveal a dramatic broadening of the auroral line of the order of 10-30 km/sec motions, with broad wings of the emission line extending out roughly ± 1 Å from line center (Clarke et al., 1989). High-resolution measurements of H Lα emission from Jupiter's aurora by the Hubble Space Telescope Goddard High-Resolution Spectrometer similarly reveal a 2Å-wide profile (Clarke et al., 1994). Multiple scattering within the line does not account for the broadened line profile (Clarke et al., 1991). These line profiles indicated a population of fast emitting H-atoms with velocities in excess of the fast atoms expected from dissociative excitation of H_2. Dissociative excitation would also be present, in view of the large number of electron collisions with H_2 revealed in [he H_2 Werner and Lyman band emissions, and an accurate measurement of the dissociative excitation line profile was needed to be able to model this component of the observed line broadening.

Unexpectedly bright UV emissions (including H Lα) were also observed from Jupiter's equatorial regions, as well as from t h e

** What is a kR? Please use SI units.

* The four outer planets are Saturn, Uranus, Neptune, and Pluto

airglows of the other giant planets (Shemansky, 1985; Clarke et al.,1987). There was initially substantial disagreement about the process by which these emissions were produced, evolving in part as a debate on the relative contributions by charged particle excitation and by solar resonance scattering and fluorescence. Specifically, Jupiter's "H Ly α bulge" emission was shown to be consistent with resonant scattering of solar Lα w th a large planetary line width, requiring a superthermal population of 5-10 km/sec H - atoms in the uppermost atmosphere. This equatorial emission feature, fixed with respect to Jupiter's magnetic field, appears bright because the planetary line is broad and scatters more of the very broad solar line, rather than due to a greatly enlarged column of H atoms. The next clear question concerns the source of the fast atoms, and dissociative excitation, again, is a candidate process. The Lα emission produced by electron collisions is limited to a small fraction of the observed emission, due to the strict upper limit to H_2 band emission, but fast H-atoms, produced high in the atmosphere, might contribute to the observed line broadening depending on the details of the velocity distribution resulting from dissociative excitation,

Detailed modeling of a planetary H Lα emission line profile requires knowledge of the kinetic energy distribution of various processes leading to a broad line profile. In this paper, w e concentrate on the analysis of the first measurement of the H Lα line profile from dissociative excitation of H_2 by electron impact.

The line profile studies of the various members of the Lyman series from dissociative excitation of H_2 leads to the determination of the kinetic energy distribution of the atomic H fragments from each dissociation limit. The uv line profiles of the higher members of the Lyman series can be modeled from detailed knowledge of the Balmer series in the visible region. However, the kinetic energy distribution function of H(2p) atoms from dissociative excitation of H_2 has not previously been measured. By analogy to line profile results, obtained from the kinetic energy distribution of H(nℓ, n=3, 4, 5) atoms, two distinct maxima in the kinetic energy distribution are expected (Ogawa and Higo, 1979; Higo et al., 1982; Nakashima et al., 1992). In addition, the kinetic energy distribution of metastable H(2s) atoms from dissociative excitation of H_2 by time-of-flight (TOF) studies has been the subject of much published research (Misakian and Zorn, 1972; Carnahan and Zipf, 1977; Spezeski et al., 1980; Ryan et al., 1972; Czuchlewski and Ryan, 1973; Leventhal et al., 1967). A

comparison of the H(2p) and H(2s) distributions is of fundamental importance in understanding the branching of the H_2 dissociation process which can occur from singly excited or doubly excited states. The former set of states leads to the "slow" component and the latter leads to the "fast" component. The Balmer-α line profile shows a characteristic narrow central peak (-300 mÅ FWHM) from the slow component and a broad wing (-1.8 Å FWHM) from the fast component. Since the Doppler displacement is proportional to wavelength, five to six times narrower line profiles can be expected in the vacuum ultraviolet (vuv) spectral region.

The Balmer line profiles have been found to be asymmetric. Further understanding of the asymmetry of the Balmer series line profiles has been accomplished by measurements of the angular intensity dependence (Nakashima et al.,. 1987) and by measurements of optical excitation functions for the wings and core of the Balmer lines (Ogawa et al., 1992). These sets of measurements give clues on the symmetries of the intermediate dissociating states. In this experiment, we provide highly sensitive first-time measurements of the H Lα line profile and the excitation functions of the H Lα line core and blue wing. We clearly see an improvement in signal-to-noise (S/N) in the vuv over H(nℓ) line profiles measurements made in the visible and time-of-flight (TOF) measurements of H(2s) excitation functions. The detailed threshold structure of H(2p) shows the appearance potential of doubly excited states contributing to the Doppler profile in the wings and contributes to a better understanding of the fast H(2s) component from experiments in the past.

The individual excitation functions are modeled by the modified Born function (Shemansky, 1985 a, b). The present results serve as a test of the cross section model that we recently developed for a lower resolution measurement of the H Lα line in which we predicted the quantum yield of fast and slow processes (Ajello et al., 1991).

EXPERIMENTAL

The experimental system has been described by Liu et al. (1995). In brief, the experimental system consists of a high-resolution 3-meter uv spectrometer in tandem with an electron impact collision chamber. A resolving power of 50,000 is achieved by

operating the spectrometer in third order. The line shapes were measured with experimental conditions that ensure linearity of signal with electron beam current and background gas pressure. All the cross sections and spectra were measured in the crossed-beam mode. The electron-impact-induced-fluorescence line profiles of H Lα at 20, 40 and 100 eV impact energy are shown in a series of spectra in Fig. 1, along with the instrumental slit function of the spectrometer. As expected at 40 and 100 eV, the line profile consists of a narrow central peak and a broad wing base. The line profile at 20 eV shows no pedestal base structure and is perfectly symmetric. However, both the 40 and 100 eV profiles are asymmetric in the peak and the wings. The 40 and 100 eV peaks are red shifted -3 mÅ from line center and the blue wing extends further from the line center than the red wing. Similar effects in Balmer-β have been studied and explained on the basis of anisotropic distribution of fragment atoms (Nakashima et al., 1987), In this experiment, the line profiles were measured at 90° both to the electron and molecular beam axes. We assume that anisotropy is small. We have acquired a vuv polarizer in our laboratory to complete the line profile asymmetry aspect of the study. Results are awaited from this experiment. In Fig. 1, the range of the measured FWHM of 44 mÅ to 49 mÅ is not narrow with respect to the instrumental slit function (FWHM =24 mÅ). Fast Fourier Transform (FFT) techniques were used to recover the actual line profile (Press et al., 1986). The measured line profile is the convolution of the true line profile and the instrumental slit function. Expressed mathematically, the measured line profile, I(λ), is given by the convolution integral

$$I(\lambda) = \int T(\lambda')\, A(\lambda - \lambda')\, d\lambda', \quad (1)$$

where $T(\lambda')$ is the true line profile at wavelength λ' and $A(\lambda - \lambda')$ is the instrumental response function. In the transform domain the convolution becomes a simple product,

$$I_T(s) = T_T(s)\, A_T(s), \quad (2)$$

where I_T, T_T, and A_T are the FFT of I, T and A, respectively and s is measured in inverse wavelength. Optimal Wiener filtering of the measured signal, I, was performed, since it includes a small noise

component (Press 'et al., 1986). Signal-to-noise ratio (S/N) is greater than 100 for all line profiles. The FFT of T is given by,

$$T_T(s) = I_T(s)\, F_T(s) / A_T(s) \quad , \qquad (3)$$

where $F(\lambda)$ is the optimal filter. We selected a step filter to remove high-frequency noise from both I_T and A-r. A small amount of "ringing" in the pedestal portion of the true line profile for 40 and 100 eV is produced by the step function and is removed by a six-point smooth. The true line profile, the measured line profile at 20 eV, and the slit function are all approximately Gaussian. The root-sum-square of the FWHM of the true line shape and the slit function should approximately equal the FWHM of the measured profile. This is found to be the case to within 2 mÅ for the 20-eV line profile, and also for the line core of the other two profiles.

LYMAN-α LINE PROFILE

We show in Fig. 2 the inverse FFT (FFT^{-1}) of $T_T(s)$ and $I_T(s)$ for the 100-eV line profile. In addition, we show the FFT^{-1} of $T_T(s)$ for the 20-eV line profile. The deconvolved line profile of the central peak is found to have a FWHM of 40 ± 4 mÅ for the 20, 40, and 100-eV H Lα line profiles. For the 100-eV line profile, the kinetic energy distribution of the fragments, P(E), is given by

$$P(E) = k(dT/d\lambda) \quad , \qquad (4)$$

where k is a multiplicative constant (Ogawa and Higo, 1979). The combined kinetic energy distributions of the fast and slow H(2p) fragments are shown in Fig. 3a for the red wing of the three line profiles of Fig. 1. Figure 3b expands the low-energy region (O-1 eV) and shows the slow fragment H(2p) kinetic energy distribution. The 20-eV results and line core results for 40 and 100 eV are achieved, without any smoothing to the FFT or to the derivative in eqn. 4. Since the measured H Lα line profiles for the central peaks at 20, 40, and 100 eV are nearly identical, it follows that the resultant slow fragment distribution for each impact energy displays the same shape. The slow fragment distribution has a FWHM of 260 ± 20 me V with a peak at 80 ± 10 meV for 20, 40, and 100-eV electron impact

energies. The results are compared to the TOF H(2s) results of Misakian and Zorn. The differences in the two results may be attributed to the loss of sensitivity in TOF experiments as the H(2s) energy approaches zero. Both sets of results indicate a high-energy cutoff at near 1 eV (Ryan et al., 1979).

Preliminary results from the combined slow and fast fragment energy distributions at 100 eV impact energy for both the red and blue wings have been previously shown (Ajello et al., 1995). The small difference in the energy distribution of the fast fragment distribution shape results from asymmetries in the line center pedestal width in Fig. 1. The fast distribution in Fig. 3a is based on four-point smoothing of P(E). Three peaks arc observed in the combined slow and fast H(2p) kinetic energy distribution. The large peak, near zero energy, from the slow atom distribution has been discussed above. The principal peak from the fast energy distribution occurs at 4 ± 0,5 eV, while the minor secondary peak occurs at 2 ± 0.5 eV. The fast peak distribution can bc compared to H(2s) results from a number of authors. The results of Spezeski et al. (1980) are nearly identical to those of Czuchlewski and Ryan (1973). Our results for H(2p) lie between the work of Misakian and Zorn (1972) and Leventhal et al. (1967) and indicate that the fast 2s and 2p atoms come from the same channels. A resolution of the fast H(2s) peak into two definite peaks at 4.4 ± 0.9 eV and ?.3 ± 0.5 eV has only been reported by Leventhal et al. (1967) at an angle of 77° with respect to the electron beam axis. This result has been disputed by results of Spezeski et al., (1980) who pointed out that no double peaks were found in their measurements or those of Misakian and Zorn. In addition, they indicated out the outstanding problem associated with the fast peak(s): What other dissociating channels beside $Q_2(^1P_u)$ autoionizing states that dissociate into H(2p,2s,1s) + H(2p,2s) contributed to this distribution? Their main evidence, that other states contribute, is a model of the changing energy dependence of the H(2s) distribution function with electron impact energy. The pedestal shapes for 40 and 100 eV are quite different, indicating a change in the fast H(2p) distribution occurs with impact energy. The maximum in the distribution function at 100 eV is 4.1 eV and the peak shifts to 3,7 eV at 40 eV.

CROSS SECTION MEASUREMENTS

The cross sections of the fast and slow H(2p) dissociation processes can be studied individually at high resolution, By placing the bandpass at line center, we obtained the excitation function of the slow H(2p) atoms. The data and the modified Born approximation model fit are shown in Fig. 4. The excitation function was put on a n absolute scale by normalizing it to the cross section value at 100 eV (5.32 x 10-'8 cm') for singly excited states leading to the slow H(2p) atoms (Ajello et al.,1991). The threshold region below 20 eV is dominated by H_2^- resonance and H_2 electron exchange processes (Ajello et al., 1991). The high-energy behavior is characteristic of a dipole allowed transition.

To obtain a measurement of the excitation function for the fast atoms, the wavelength position of the spectrometer was offset from the line center. By placing the center of the bandpass on the blue wing 104 mÅ from the line center and restricting the FWHM of t h e bandpass to 36 mÅ established a data set that clearly shows the threshold(s) for the fast processes. The excitation function for the blue wing is shown in Fig. 5 for the threshold region. Fig. 6 shows the excitation function in the electron impact range 0-200 eV, along with the modified Born model. The slow and fast data, described herein, are fitted within experimental error using analytic cross sections having the modified Born form

$$\Omega_{ij} = co\ (1\text{-}1/x)\ (x'') + \sum_{k=1}^{4} C_K\ (X\text{-}1)\ \exp(-kC_kX) + C_5 + C_6/X + C,\ in(X), \quad (5)$$

where Ω_{ij} (X) is the collision strength, X is the electron energy i n threshold units, and the C_k are constants of the function (Shemansky et al., 1985a, b). The excitation cross section is given by the equation

$$\sigma_{ij} = \Omega_{ij}(X)(E_{ij}\ X), - ' \quad (6)$$

where σ_{ij} is the cross section in atomic units and E_{ij} is the transition energy in Rydberg units.

Four thresholds were identified as shown in Fig. 5. The first threshold at 16.67 eV must correspond to singly excited states tied to the H(1 s)+ H(3p,3s) dissociation limit. Cascade from Hα contributes t o the line profile above 16.67 eV. Blue light, a leak from the base of the signal from the central peak, might be the reason for the slow

atom contribution to the blue wing. Higo et al, (1982) find the slow atom distribution for $H_2(n\geq 3)$ to be broader than for n=2, above.

The other three thresholds can be attributed to doubly excited states of H_2 which have the lowest $^2\Sigma_u^+$ and first excited $^2\Pi_u$ states of H_2^+ as core orbitals. They are designated Q_1 and Q_2, respectively (Guberman, 1983). The fundamental calculations by Guberman (1983) allowed us to identify where the Q_1 and Q_2 states cross the right hand edge of the Franck-Condon region. The most closely aligned thresholds of Guberman are associated with the measurement. In some cases more than one threshold lies within 0.5 eV of the measurement uncertainty. For the first time, from detection of 2ℓ states, doubly excited states of H_2 are observed at the lowest dissociation threshold of 23.0 eV. According to Guberman, the **$Q_1(^1\Sigma_g^+(1))$** state is the responsible state. The next threshold at 27.63 eV can arise from the $Q_1(^1\Sigma_g^+(2))$ state (at 27.2 eV), $Q_1(^{3,1}\Pi_g(2))$ states (at 27.4 eV and 27.5 eV), or/and $Q_1(^{3,1}\Pi_u(2))$ states (at 27.5 and 27.6 cV). However, the selection rules for molecular dissociation do not allow any of the Π_g transitions (Dunn, 1963). The final sharp threshold in Fig. 5 at 29.92 eV correlates with a set of $Q_2(^1\Sigma_g^+, ^{1,3}\Pi_u)$ states between 30 and 32 eV. Thus, many dissociation channels contribute to the fast atom dissociation process as predicted by Spezeski et al (1980). The steep rise in cross section, beginning at 30 eV, verifies that the dominant contribution to the fast H(2p) distribution comes from the $Q_2(^1\Sigma_g^+, ^1\Pi_u)$ states as previously concluded for H(2s) (Misakian and Zorn, 1972).

The plot of the cross section in Fig. 6 indicates an optically forbidden process. The shape is indicative of the two; electron excitation process required for doubly excited states. The modified Born approximation model is given in Table 1 and includes two thresholds, one each for the Q_1 and Q_2 states, at 23.0 and 30.2 eV (Guberman, 1983), respectively. The models in Table 1 show that the two cross sections are assumed to have the same energy dependence with 40 % of the cross section arising from the Q_1 state(s) and 60 % attributed to the Q_2 state(s). The strength of the threshold behavior of the two processes from the data in Fig. 5 and Fig. 6 clearly demonstrates the dominance of the Q_2 cross section.

The ratio of the fast to slow cross section is shown in Fig. 7 and peaks at 100 eV. It has been concluded in our experiment that the ratio falls sharply after 200 eV. Thus the quantum yield of fast atoms peaks at 100 eV. Integrating under the kinetic energy

distribution in Fig. 4 gives a fractional percentage of 0.69 and 0.31, for the slow and fast atoms, respectively. This result can be compared to the low; resolution 100 eV cross section budget from our laboratory (Ajello et al., 1991). This budget predicted that the partitioning of dissociation from slow atoms and fast atoms occurred with a fractional percentage of 0.73 and 0.27, respectively. This agreement within the 5% experimental error bars for the fractional ratio testifies to the usefulness of the modified Born technique developed by Shemansky et al. (1985a,b) for dissecting low resolution excitation functions consisting of distinct processes. The slow/fast atom quantum yield at 100 eV is quite different than that found for H(2s) by Carnahan and Zipf (1977). Their measured fractional percentages are 0.87 and 0.13, respectively.

DISCUSSION

The H Lα line profile resulting from dissociative excitation of H_2 reported here provides the information needed to include this process in models of the production of Jupiter's auroral and equatorial H Lα emission line profiles. Additionally, in both cases the fast H-atoms resulting from dissociative excitation can enhance the planetary emission through resonant scattering in the wings of the broad solar line. The experimental H Lα line width reported here suggests that the fast atom population resulting from dissociative excitation is not sufficient, by itself, to explain the observed line broadening on Jupiter. However, this is one contributing process in the production of the auroral and equatorial Lα "bulge" emissions and the observed Doppler-broadened line profiles.

The H Lα line from dissociative excitation of H_2 is much broader than the thermal Doppler absorption line profile for H Lα from atomic H in the Jovian atmosphere. The radiative transfer of the wings of H Lα from dissociative excitation is essentially optically thin for an atmosphere thick in atomic H. A small wavelength region within ~75 mÅ of line center, dependent on foreground abundance, would be affected by atomic H absorption and multiple scattering (Clarke et al.,1991).

Within experimental uncertainty of approximately 0.5 eV, the kinetic energy distributions of the fast H(2s) and H(2p) atoms appear to be identical from 2 to 10 eV. Some H(2p) structure is indicated near 7 cV, which has been partially attributed to the second and

higher Q_1 states. Further line profile work via polarization studies and at emission angles other than 90° is needed to understand the secondary peak in the neighborhood of 2 eV. One possible explanation for this peak is the relative importance of cascade from higher Rydberg states for the fast-atom contribution. We did observe a threshold precisely at 16.7 eV from cascade. Our analysis shows a contribution of 25% to the fast, atom population of H(2p), whereas H(2s) atoms contain only a 4% contribution (Ajello et al., 1991). The superthermal energy released into the atmosphere by the doubly excited states can be calculated ~~by~~ from the cross sections provided by this work.

Above the threshold of singly excited states at 14.7 eV, the importance of singly excited triplet states in the slow - atom distribution is evident in the rapid rise of the cross section, The importance of the various singlet anti triplet states has been described elsewhere (Ajello et al., 1991). Compared to singlet states, the triplet states such as e $^3\Sigma_u^+$ make a greater contribution to the H(2p,2s) slow-atom cross section production at threshold.

Figure 8 shows a schematic of the potential energy curves for H_2 labeled with the important singly and doubly excited states. The kinetic energy distribution is shown for the three processes found in this study. The slow H(2p) atoms can arise from direct excitation to dissociating or predissociating states. At 100 eV, the most important singly excited state contributors to slow atom H(2p) production arc direct dissociation of the B' $^1\Sigma_u^+$ state and predissociation of the B", D and D' states by the B' state (Ajello et al., 1991). There is also a small contribution to the slow-atom distribution function from Hα cascade at 16.56 CV excitation energy corresponding to the H(3ℓ) + H(1s) dissociation imit. A schematic of the fast-atom distribution for the first $Q_1\,^1\Sigma_g^+$ state is shown. The asymptotic limit for the Q, $^1\Sigma_g^+$ doubly excited state is 14.68 eV, while the inner part of the right-hand edge of the Franck-Condon region occurs at 23 CV (Guberman, 1983). The left-hand edge of the Franck-Condon region stretches to about 32 cV. The peak of the distribution occurs in the middle of the region (-27-28 eV). The most probable energy for the fast H(2p) atoms is 4-5 eV. Similar distribution functions arise from the $Q_2(^1\Sigma_g^+, ^1\Pi_u)$ states but would lie 6-10 CV above the H(2s,2p) + H(2s,2p) asymptote at 24.9 eV. The Franck-Condon region for the Q_2 states would encompass the region from 30 to 40 CV on the potential energy diagram. The Q_2 states are the most important set of doubly

excited states, producing upon dissociation pairs of fast 2p and 2s products. These atomic H products maybe the source of important physical chemistry in the outer planets.

ACKNOWLEDGMENTS

The research described in this text was carried out at the Jet Propulsion Laboratory, California Institute of Technology. The. work was supported by the Air Force Office of Scientific Research (AFOSR), the Aeronomy Program of the National Science Program (grant ATM-9320589 to the University of Southern California) , and NASA Planetary Atmospheres, Astronomy/Astrophysics and Space Physics Program Offices. S. M. Ahmed is supported by a National Research Council Resident Research Associateship. We acknowledge important discussions with and careful review of the manuscript by S. Trajmar, D. Shemansky, W. McConkey, G. Dunn, G. Lawrence and T. Ogawa.

REFERENCES

Ajello, J. M., S. M. Ahmed, I. Kanik, and R. Multari, Kinetic energy distribution of H(2p) from dissociative excitation of H_2, Phys. **Rev** Lett., in press, 1995.

Ajello, J. M., D. E. Shemansky , and G. K. James, Cross sections for production of H(2p,2s,ls) by electron collisional dissociation of H_2 *Ap. J.*, 371, 422-431,1991.

Broadfoot, A. L. et al., Extreme ultraviolet from Voyager 1 encounter with Jupiter, Science, 204, 979-982, 1979.

Broadfoot, A. L, et al., Ultraviolet spectrometer observations of Uranus, Science, 23.?, 74-79, 1986.

Broadfoot, A. L. et al., Ultraviolet spectrometer observations of Neptune and Triton, Science, 246, 1459-1466, 1989.

Carnahan, B. L. and E. C. Zipf, Dissociative excitation of H_2, HD and D_2 by electron impact, *Phys.* Rev. *A,* 16, 991-1002, 1977.

Clarke, J. T., L. Ben Jaffel, A. Vidal-Madjar, G. R. Gladstone, J. H. Waite, R. Prange, J. Gerard, J. Ajello, and G. James, Hubble Space Telescope Goddard High Resolution Spectrometer H_2 rotational spectra of Jupiter's aurora, *Ap. J. Lett.*, 430, L73-L76, 1994.

Clarke, J. T., G. R. Gladstone, and L. Ben Jaffel, Jupiter's dayglow H Lyα emission line profile, *Geophys. Res. Left.,]* 8, 1935-1938, 1991.

Clarke, J. T., M. K. Hudson, and Y. L. Yung, The excitation of the far-ultraviolet electroglow emissions from Uranus, Saturn and Jupiter, *J. Geophys. Res.,* 92,15139, 1987.

Czuchlewski, S, J. and S. R. Ryan, Collisional quenching of metastable hydrogen atoms by noble gases, *Bull. Am. Phys. Soc.,* 18, 688, 1973.

Dunn, G. H., Anisotropies in angular distributions of molecular dissociation products, *Phys. Rev. Lett. 8, 62-64, 1963.*

Guberman, S. L., Autoionizing states of H_2, *J. Chem. Phys.,* 78, *1404-*1413, 1983.

Higo, M., S. Kamata and T. Ogawa, Electron impact dissociation of molecular hydrogen and deuterium: translational energy distribution of atomic hydrogen and deuterium (n = 3,4,5), *Chem. Phys.,* 66, *243-248, 1982.*

Ito, K., N. Oda, Y. Hatano, and T. Tsuboi, Doppler l'refile of Balmer-α radiation by electron impact, *Chem. Phys., 17, 35-43, 1976.*

Leventhal, M., IL-T. Robiscoe, and K. R. Lea, Velocity distribution of metastable H atoms produced by dissociative excitation of H_2, *Phys.* Rev., 158, 49-56, 1967.

Liu, X., S. M. Ahmed, J. M. Ajello, G. K. James, R. Multari, H. Hu, and D. E. Shemansky, High resolution electron impact spectrum of molecular hydrogen, *Ap. J. Supp.*, In Press ,1995.

Misakian, M, and J. C. Zorn, Dissociative excitation of molecular hydrogen by electron impact, *Phys. Rev. A , 6, 2180-2196, 197, 1972.*

Nakashima, K., M. Tanguchi, and T. Ogawa, Electron impact dissociation of hydrogen molecule. Time resolved measurements of the Balmer line, *Chem. Phys. Lett., 197, 72-76,* 1992.

Nakashima, K., H. Tomura, and T. Ogawa, Symmetry of the dissociation of hydrogen: angular dependence of the excited hydrogen atom (n=4) produced in e-H_2 collisions, *Chem. Phys. Lett.*, 138, *575 -578, 1987.*

Ogawa, T. and M. Higo, Analysis of the translational energy distribution of H* produced in the e-H_2 collision, *Chem. Phys. Lett.*, 65, 610-612, 1979.

Ogawa, T. and M. Higo, Translational energy distribution and production mechanism of excited hydrogen atoms by controlled electron impact on H_2, *Chem. Phys.*, 52, 55-64, 1980.

Ogawa, T., S. Ihara, and K. Nakahima, Fano plots for the slow and fast groups of excited hydrogen atoms produced in e-H_2 collisions, *Chem. Phys. Lett.*, 161, 509-513, 1992.

Press, W. H., B. P. Flannery, S. A. Teukolsky, and W. T. Vettering, *Numerical Recipes* (Cambridge University Press, Cambridge, England, 1987)

Ryan, S. R., J. J. Spezeski, O. F. Kalman, W. E. Lamb, L. C. McCyntyre, and W. H. Wing, Time of flight study of H(2s) and D(2s) by electron impact on H_2, D_2 and HD: Evidence for predissociation, *Phys. Rev. A, 19, 2192-2196, 1979.*

Shemansky, D. E., An explanation for the H Lyα longitudinal asymmetry in the equatorial spectrum of Jupiter: an outcrop of paradoxical energy deposition in the exosphere, *J. Geophys. Res.*, 90, 2673, 1985.

Shemansky, D. E., J. M. Ajello, D. T, Hall, electron impact excitation of H_2: Rydberg band systems and the benchmark cross section for H lyman-alpha, *Ap. J.*, 296, 765-773, 1985a.

Shemansky, D. E., J. M. Ajello, D. T. Hall, and B. Franklin, Vacuum ultraviolet studies of electron impact of Helium: Excitation of He n^1P^0 and ionization excitation of He^+ nl rydberg series, ***Ap.*** *J.*, 296, 774-783,

1985b.
Spezeski, J. J., O. F. Kalman, and L. C. McCyntyre, Time of flight **study** of H(2s) and D(2s) produced by electron impact on H_2 and D_2: Fast peaks, *Phys. Rev. A*, 22, 1906-191, 1980.

COLLISION STRENGTH COEFFICIENTS FOR $e + H_2 \rightarrow H\ L\alpha$

TABLE I

i	%	E_{ij}	C_0	C_1	C_2	C_3	C_4	C_5	C_6	C_7	C_8
1	***100***	***14.67***	***0.80040***	0.14727	-0.00592	0.01464	0.40418	-1.1253	1.1253	0.53674	0.14454
2	40	23.0	-.067 84	0.034857	-0.099768	0.50682	-0.92647	0.20852	-0.20852	0.0	0.25704
3	60	30.2	SAME	AS	i=2						

TABLE OF FIGURES

FIGURE 1. Experimental spectra: (a) 100 eV H Lα line profile; (b) 20-eV H Lα line profile; (c) zero -order slit function of experimental apparatus scaled to third order; (d) 40 -eV H Lα. The data statistics were better than 1% in a), b), and c). The wavelength step size i n third order was 2.667 mÅ. The operating conditions, were established as follows: (1) background gas pressure of 1×10^{-4} torr and (2) electron beam current of 269 mÅ. Peak signal was 13000, 9000, and 6000 counts in the 100- eV, 40- eV, and 20- eV line profiles, respectively, with background signals of under 100 counts. The FWHM of the 100- eV, 40-eV, 20-eV, and instrument slit function are 47 mÅ, 44 mÅ, 49 mÅ, and 24 mÅ, respectively.

FIGURE 2. Deconvolution of 20- and 100- eV line profile data along with the inverse FFT of the FFT of the data in Fig. 1a.

FIGURE 3a. Fast H(2p) atom kinetic energy distribution function compared to work of Misakian and Zorn (1972).

FIGURE 3b. Kinetic energy H(2p) distribution of slow atoms at 20 and 100 eV compared to work of Misakian and Zorn (1972). The distributions arc obtained from Fig. 1 as explained in the text using FFT techniques.

FIGURE 4. Absolute cross section of the H(2p) slow component from an excitation function measurement of the line core of H Lα. The bandpass of the spectrometer is 24 mÅ. The modified Born approximation model constants are given in Table 1.

Figure 5. Optical excitation function of H Lα line blue wing. The u v bandpass is offset 104 mÅ from line center. The bandpass is set a t 3 6 mÅ FWHM. The Appearance Potentials (AP) of various dissociation channels are found by modeling the linear behavior of the cross section near threshold. The channel spacing is 20 meV. The electron gun energy resolution is 300 meV.

FIGURE 6. Absolute cross section of the H(2p) fast component from an excitation function measurement of the blue wing centered 104 mÅ from line center. The bandpass of the spectrometer is 36 mÅ. The modified Born approximation model constants are given in Table 1 of H Lα.

FIGURE 7. Ratio of cross sections of fast H(2p) component to slow H(2p) component from model of Fig. 4 and Fig. 6.

FIGURE 8. Partial potential energy diagram of H_2 showing the singly excited and doubly excited states (Ajello et al., 1991). The inserts are a schematic of the fast and slow dissociation processes.

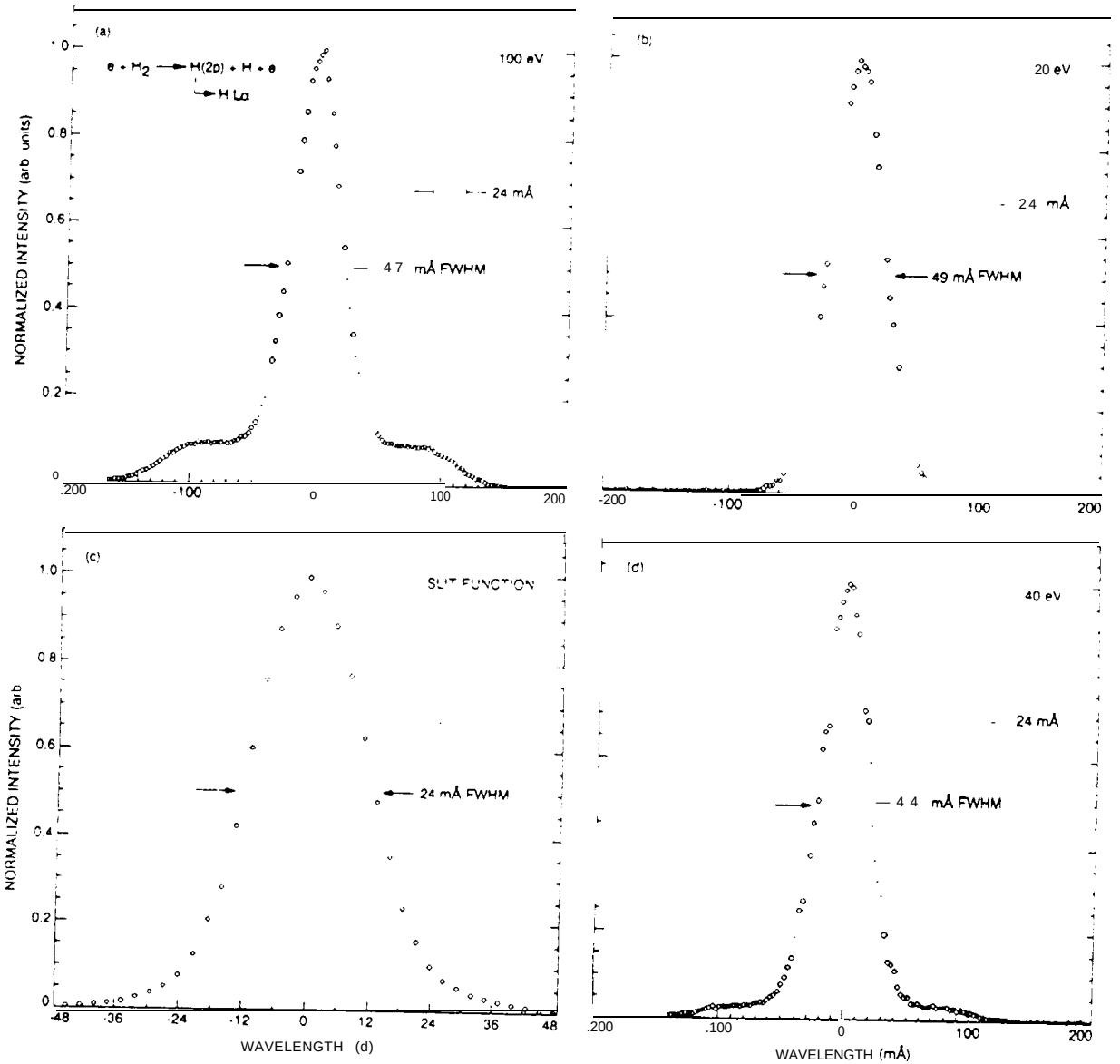
(a)
100 eV
e + H2 → H(2p) + H + e
→ H Lα
24 mÅ
47 mÅ FWHM
NORMALIZED INTENSITY (arb units)
(b)
20 eV
24 mÅ
49 mÅ FWHM
(c)
SLIT FUNCTION
24 mÅ FWHM
NORMALIZED INTENSITY (arb
WAVELENGTH (d)
(d)
40 eV
24 mÅ
44 mÅ FWHM
WAVELENGTH (mÅ)

Fig. **1**

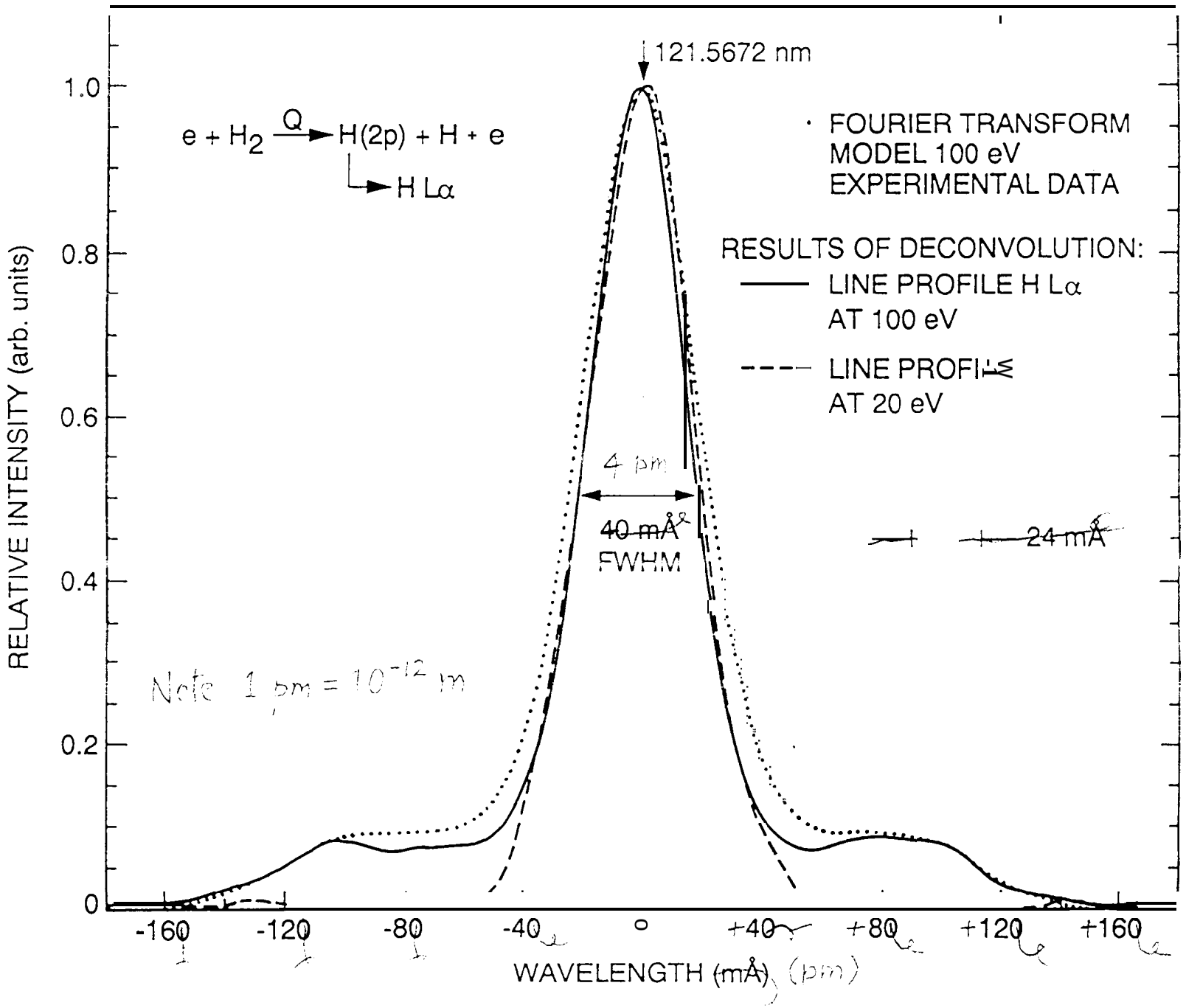
121.5672 nm
e + H2 → Q → H(2p) + H + e
H Lα
FOURIER TRANSFORM
MODEL 100 eV
EXPERIMENTAL DATA
RESULTS OF DECONVOLUTION:
LINE PROFILE H Lα
AT 100 eV
LINE PROFILE
AT 20 eV
4 pm
40 mÅ
FWHM
24 mÅ
Note 1 pm = 10^-12 m
RELATIVE INTENSITY (arb. units)
1.0
0.8
0.6
0.4
0.2
0
-160
-120
-80
-40
0
+40
+80
+120
+160
WAVELENGTH (mÅ) (pm)

Fig. 2

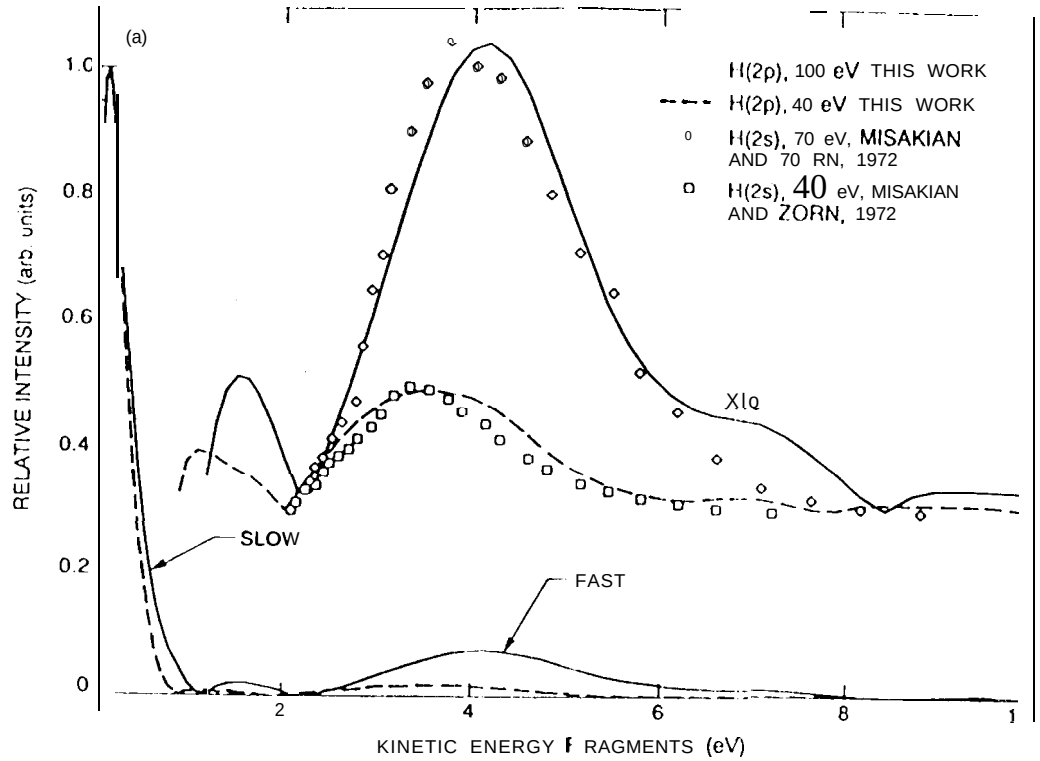
(a)
H(2p), 100 eV THIS WORK
H(2p), 40 eV THIS WORK
H(2s), 70 eV, MISAKIAN AND 70 RN, 1972
H(2s), 40 eV, MISAKIAN AND ZORN, 1972
RELATIVE INTENSITY (arb. units)
SLOW
FAST
KINETIC ENERGY F RAGMENTS (eV)

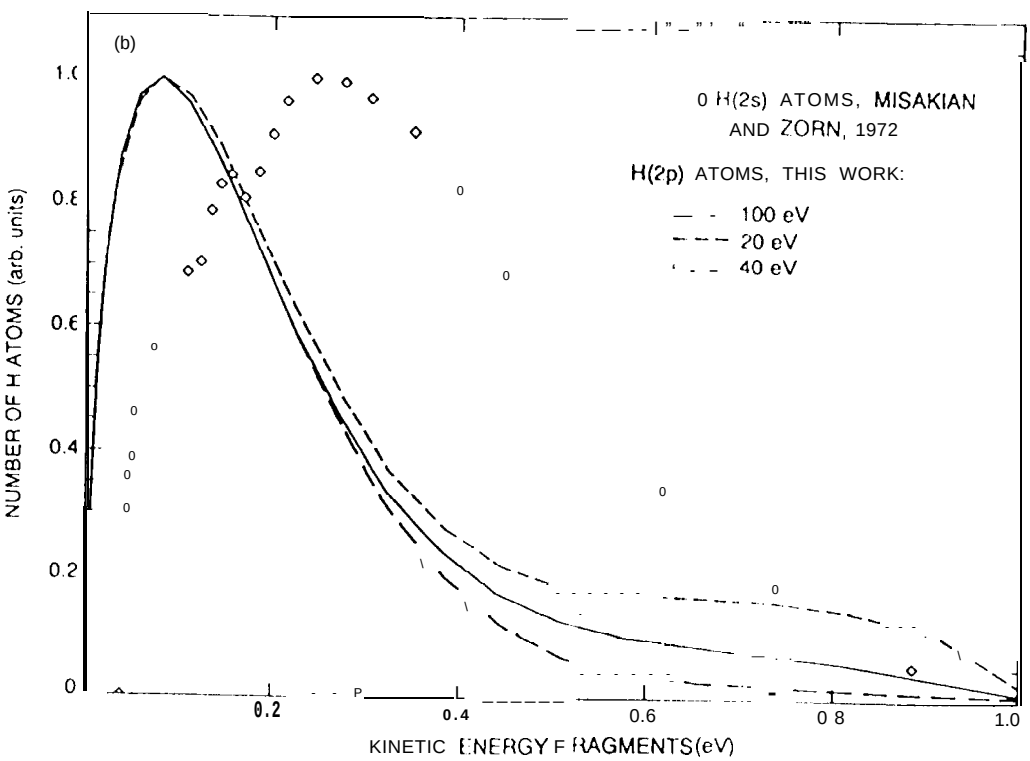
(b)
0 H(2s) ATOMS, MISAKIAN AND ZORN, 1972
H(2p) ATOMS, THIS WORK:
100 eV
20 eV
40 eV
NUMBER OF H ATOMS (arb. units)
KINETIC ENERGY F RAGMENTS (eV)

Fig. 3

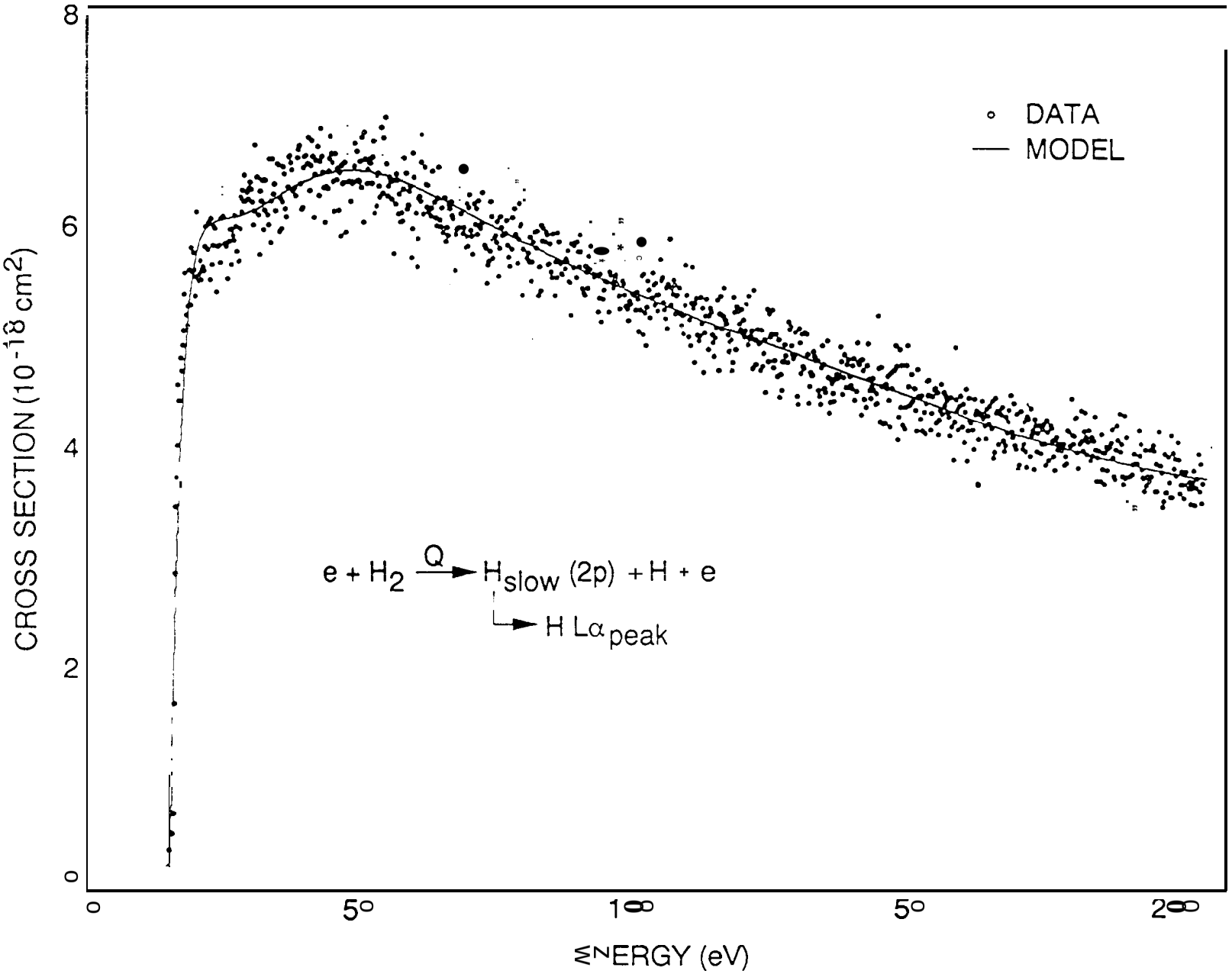
8
6
4
2
0
CROSS SECTION (10^{-18} cm^2)
DATA
MODEL
$e + H_2 \xrightarrow{Q} H_{slow}(2p) + H + e$
$\hookrightarrow H\ L\alpha_{peak}$
0
5o
1oo
5o
2oo
ENERGY (eV)

Fig. 4

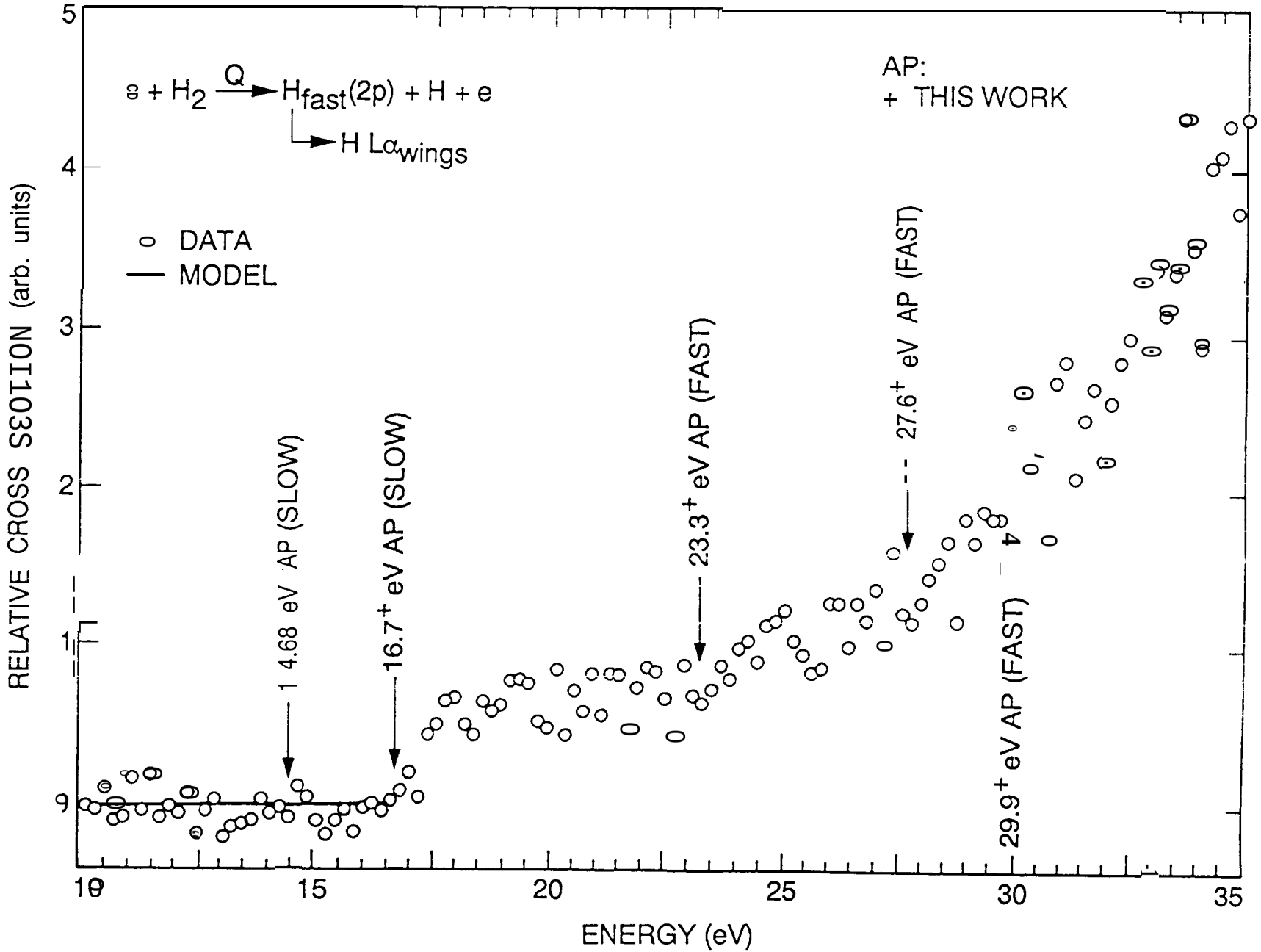
s + H2 → Q → Hfast(2p) + H + e
H Lα wings
AP:
+ THIS WORK
o DATA
— MODEL
RELATIVE CROSS SECTION (arb. units)
14.68 eV AP (SLOW)
16.7+ eV AP (SLOW)
23.3+ eV AP (FAST)
27.6+ eV AP (FAST)
29.9+ eV AP (FAST)
ENERGY (eV)
10
15
20
25
30
35
1
2
3
4
5

Fig. 5

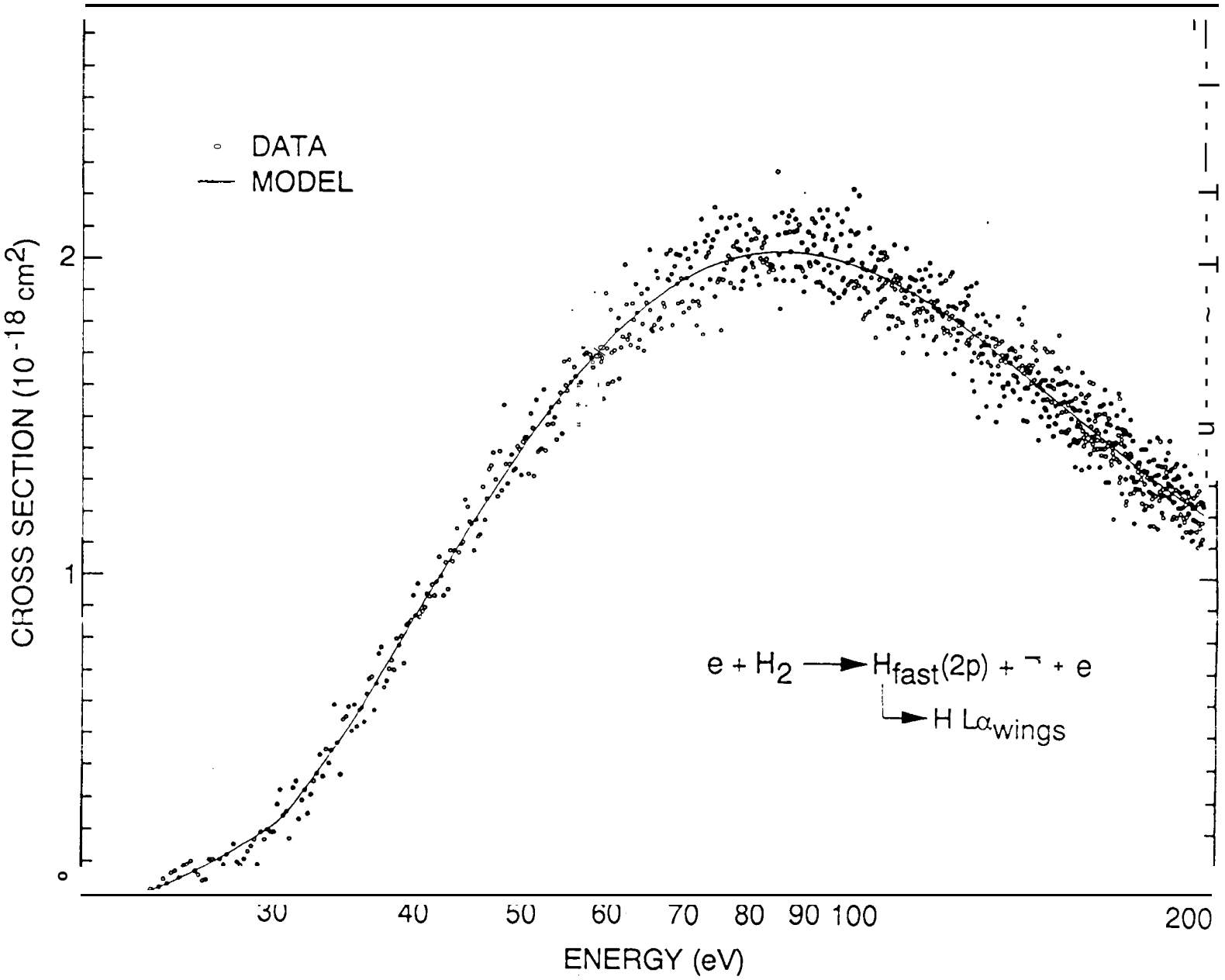
DATA
MODEL
CROSS SECTION (10^{-18} cm^2)
0
1
2
30
40
50
60
70
80
90
100
200
ENERGY (eV)
$e + H_2 \rightarrow H_{fast}(2p) + \neg + e$
$\hookrightarrow H\ L\alpha_{wings}$

Fig. 6

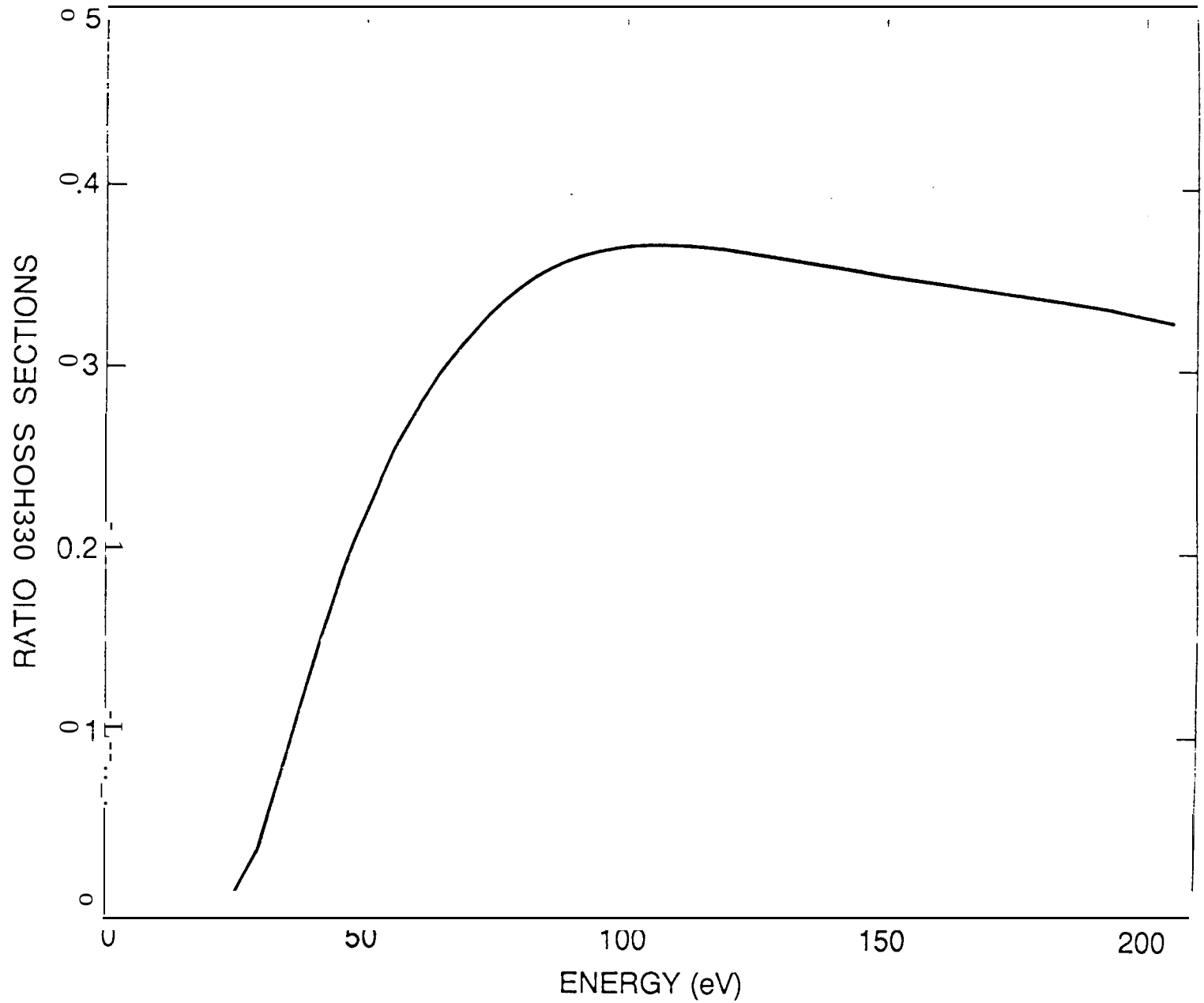
RATIO OF ENERGY LOSS SECTIONS
0.5
0.4
0.3
0.2
0.1
0
0
50
100
150
200
ENERGY (eV)

Fig. 7

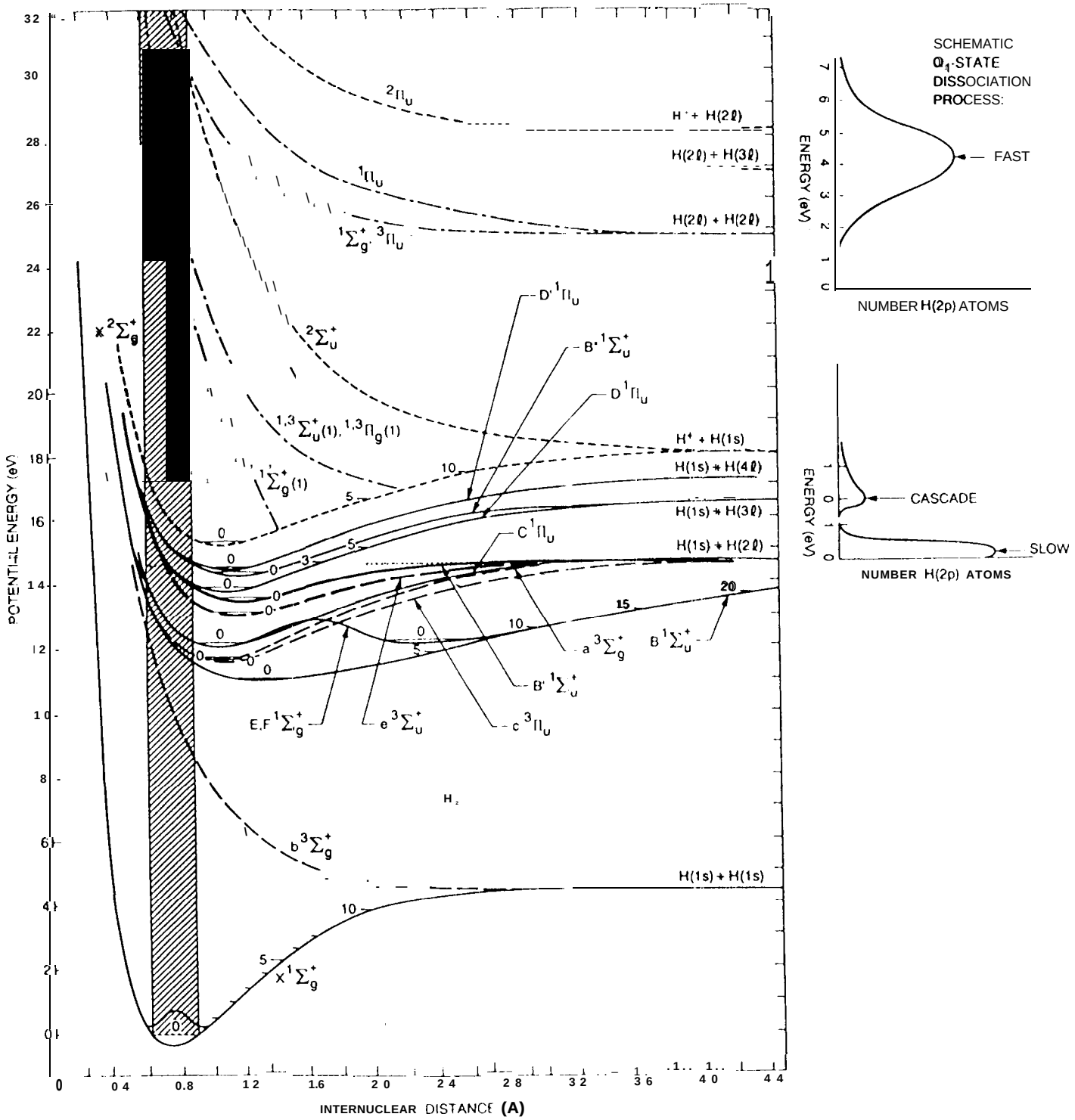
POTENTIAL ENERGY (eV)
INTERNUCLEAR DISTANCE (A)
H₂
H⁺ + H(2ℓ)
H(2ℓ) + H(3ℓ)
H(2ℓ) + H(2ℓ)
H⁺ + H(1s)
H(1s) + H(4ℓ)
H(1s) + H(3ℓ)
H(1s) + H(2ℓ)
H(1s) + H(1s)
$^2\Pi_u$
$^1\Pi_u$
$^1\Sigma_g^+, ^3\Pi_u$
$X^2\Sigma_g^+$
$^2\Sigma_u^+$
$^{1,3}\Sigma_u^+(1), ^{1,3}\Pi_g(1)$
$^1\Sigma_g^+(1)$
$D'^1\Pi_u$
$B'^1\Sigma_u^+$
$D^1\Pi_u$
$C^1\Pi_u$
$a^3\Sigma_g^+$
$B^1\Sigma_u^+$
$B'^1\Sigma_u^+$
$E,F^1\Sigma_g^+$
$e^3\Sigma_u^+$
$c^3\Pi_u$
$b^3\Sigma_g^+$
$X^1\Sigma_g^+$
SCHEMATIC
Q_1-STATE
DISSOCIATION
PROCESS:
ENERGY (eV)
FAST
NUMBER H(2p) ATOMS
CASCADE
SLOW
NUMBER H(2p) ATOMS

Fig. 8